School on the Physics of Equatorial Atmosphere

(24 September - 5 October 2001)

Gravity Waves

R. A. Vincent

(University of Adelaide)

1   Introduction

Waves usually produce small perturbations in the basic atmospheric parameters such as wind and temperature. How do we determine the perturbation quantities and interpret them in terms of useful wave parameters, such as frequency, propagation direction and so on? In addressing these issues it must also be recognized that observational selection is a significant problem. Different techniques are sensitive to different parts of the wave spectrum; no one technique can provide all the information that is necessary to fully characterize the wave field.

2   Basic Wave Parameters

Observations provide information on wave perturbations in wind, temperature, density etc. Ideally, one would like simultaneous, continuous measurements taken with high time and height resolution of the three-dimensional wind velocity (u, v, w) and temperature T over as wide a range of heights as possible. Unfortunately, virtually no instrument is capable of making such measurements, although very specialized wind/temperature lidars are becoming available (Gardner and Yang, 1998). Observations made with different techniques need to be compared and combined in order to assess the role of waves in determining the state of the atmosphere. Some techniques, such as radiosondes and rockets, provide nearly instantaneous vertical profiles of horizontal wind and temperature over a wide height range (e.g. see Figure 2). Other methods, such as radars, provide wind measurements with good time coverage, but not always over a wide height range. Once the data are acquired, and by whatever technique, there is a need to reduce the data in some commonly accepted manner so that they can be compared. It is useful to represent or parameterize the data so that they can be incorporated in numerical circulation models of the atmosphere Different model parameterization schemes represent waves in different ways, but basically the need is for information on one or all of the following:

- Wave amplitudes or energy as a function of time and space.

- Propagation directions in the both the horizontal and vertical.

- The relative importance of different wave sources.

- Wave energy and momentum fluxes as a function of frequency and wavenumber.

2.1 Wave energy

An observed variable can be represented as a perturbation ($'$) superimposed on a basic state $\overline{()}$. In the following, the zonal, meridional, and vertical wind components, and temperature are, respectively, denoted by $\overline{u} + u'$, $\overline{v} + v'$ $\overline{w} + w'$ and $\overline{T} + T'$. An important problem in data analysis is deciding how to determine and remove the background state. One way is to high-pass filtered in either wavenumber or frequency space. This requires a judgment as to what constitutes a suitable cut-off wavenumber or frequency to remove non-wave components. Figure 1 illustrates the process for GPS/MET observations of temperature. Sometimes it is more convenient to fit and subtract a low-order polynomial (Figure 2). Whatever the situation, some degree of bias will be introduced into the wave determination due to the choice of filter or polynomial (e.g. Vincent et al., 1997).

After the perturbation or fluctuating components have been obtained the wave energy per unit mass can be computed:

$$E = \frac{1}{2} \left(\overline{u'^2} + \overline{v'^2} + \overline{+w'^2} + \frac{g^2 \overline{\hat{T}'^2}}{N^2} \right) \tag{1}$$

where $\hat{T}' = T'/\overline{T}$ is the perturbation temperature normalized to the background temperature, g is the acceleration due to gravity and N is the buoyancy frequency. In (1) terms involving velocity components constitute the kinetic energy (KE) and the term involving T is the potential energy (PE). In practise w' is much smaller than either u' or v', so $\overline{w'^2}$ can be neglected.
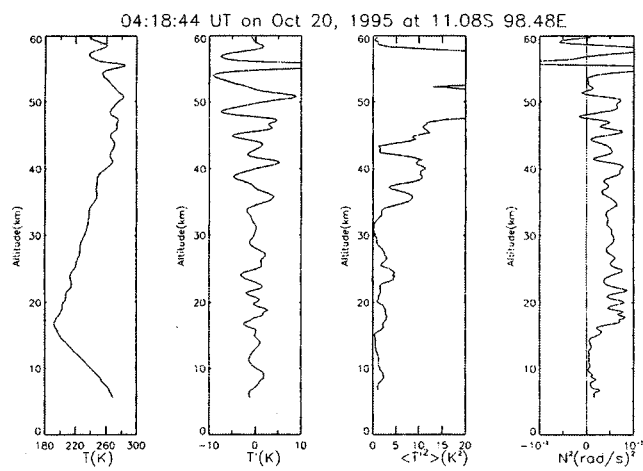
Figure 1: GPS/MET temperature profiles obtained at (11°S, 99°E), October 20, 1995. The panels show left to right the temperature profile, the temperature fluctuations after the high-pass filtering with a cut-off of 10km, temperature variance in 2km layers, and the square of the buoyancy frequency, N^2 (after Tsuda et al., 2000)
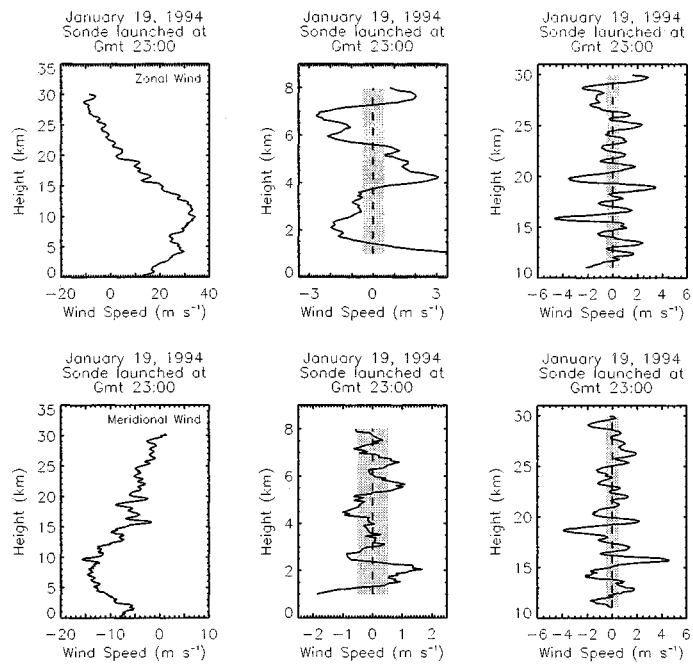
Figure 2: Zonal (top) and meridional (bottom) wind speed and fluctuations observed by radiosonde over Macquarie Island. Data from height ranges in the troposphere (middle) and stratosphere (right) are shown. The background values were determined by fitting third-order polynomials in the 2-9 km and 17-24 km height ranges.

A time series of monthly mean wave energy is shown in Figure 3. Derived from six years of routine radiosonde data taken in the Cocos Islands (12°S, 97°E) it shows an annual cycle in energy, with maximum values observed at the time of year when convection is strongest. There is also quasi-biennial variation, which is related to the phase of the QBO in mean winds. This raises the question: Are the annual and QBO-like variations due to sources or wind-filtering effects? Vincent and Alexander (2000) and Alexander and Vincent (2000) discuss these issues further.
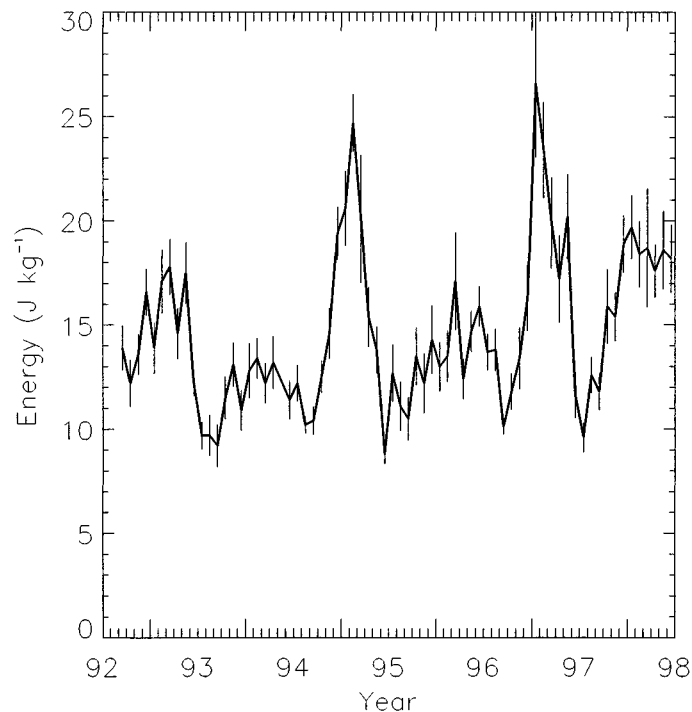
Figure 3: Time series of monthly-mean wave energy per unit mass averaged over the 18-25 km height range.

Radiosondes provide much of the basic information used for studies of gravity waves in equatorial troposphere and lower stratosphere. If high-vertical resolution wind and temperature data are available then they can be used to develop climatologies of wave activity. Routine soundings made by

weather services are an important resource currently used in an international project coordinated by the WCRP project *Stratospheric Processes and their Role in Climate* (SPARC) to develop a global climatology of gravity wave parameters.

Where temperature-only data are available then the potential energy (PE) can be used to assess wave amplitudes. Allen and Vincent (1995) used high resolution radiosonde data to develop a wave climatology in the troposphere and stratosphere for the Australian region. Tsuda et al (2000) derived a more global PE climatology in the stratosphere from temperatures acquired with GPS occultation observations, as shown in Figure 4. Temperature perturbations are largest at low latitudes and seem to be linked to tropical convection sources.
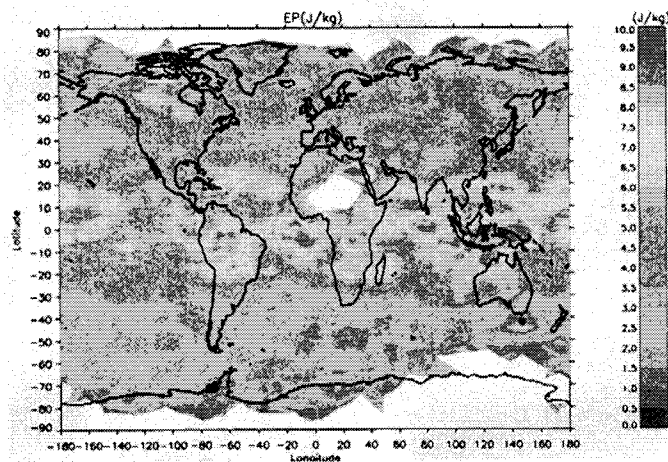

Figure 4: Global distribution of PE

3 Propagation Directions

Gravity waves may be propagating in preferred directions in both the vertical and horizontal. Wave sources may radiate waves in anisotropically, while waves propagating through a background that changes with height may be

removed at critical levels where their phase speed equals the background wind (wind-filtering). It is important to quantify the degree of anisotropy.

Consider the polarization relations that relate the various fluctuations induced by an idealized monochromatic gravity wave propagating in an isothermal atmosphere with constant wind. If fluctuations are harmonic in time and space $u', v', w', T' \sim e^{i(kx+ly+mz-\hat{\omega}t)}$, then v' is expressed in terms of u' as

$$v' = \frac{\hat{\omega}l - ifk}{\hat{\omega}k + ifl}u'. \tag{2}$$

Here f is the local inertial frequency and $\hat{\omega}$ is the intrinsic frequency, the wave frequency measured in a reference frame moving with the background wind. The vertical wavenumber m is related to the horizontal wavenumbers k, l, through the non-hydrostatic dispersion relation

$$m^2 = \frac{N^2 - \hat{\omega}^2}{\hat{\omega}^2 - f^2}k_h^2 - \frac{1}{4H^2} + \frac{\hat{\omega}^2}{c_s^2} \tag{3}$$

where $k_h^2 = k^2 + l^2$, H is the density scale height and c_s is the speed of sound. Usually, it is possible make the so-called Boussinesq approximation $(m > 1/2H)$ and ignore the last two terms in (3), so that

$$m = \pm\sqrt{\frac{N^2 - \hat{\omega}^2}{\hat{\omega}^2 - f^2}}k_h. \tag{4}$$

Downward phase velocity $(m < 0)$ is associated with upward group velocity and hence upward energy propagation.

The perturbation wind vector is elliptically polarized. In the limit as $\hat{\omega} \to f$ the polarization becomes circular and as $\hat{\omega} \to N$ it becomes linear. For waves propagating energy upward the vector rotates in an anticyclonic manner with increasing height i.e. clockwise in the northern hemisphere $(f > 0)$ and anticlockwise in the southern hemisphere. Figure 5a illustrates the hodograph of a wave with $\hat{\omega} = 2f$.

3.1 Vertical energy propagation

A simple way to determine the mean direction of propagation is to examine the sense of rotation of hodographs after the mean winds have been removed.
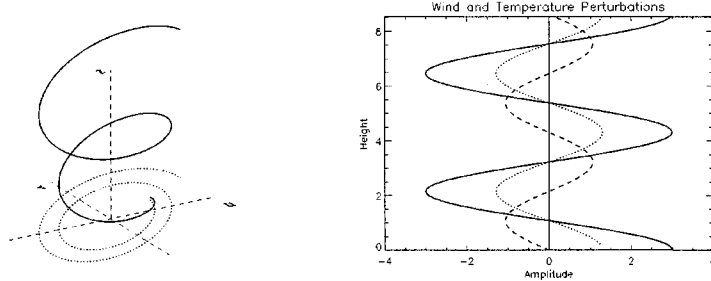
Figure 5: a: Perturbation wind profile as a function of height (solid line) for an idealized gravity wave with $\hat{\omega} = 2f$. The dotted line is the projection of the hodograph onto the horizontal plane (left panel). b: Vertical profiles of $u'_{\parallel}$ (solid), w' (dotted), and T' (dashed) for a wave propagating to the right and upward (right panel).

Where many observations are available the "rotary decomposition" technique provides a more statistical approach (e.g. Vincent, 1984). Defining the complex wind vector as

$$V'(z) = u'(z) + iv'(z) = ae^{-imz} \tag{5}$$

and Fourier transforming $V'(z)$ gives $\mathcal{A}(m)$ in vertical wavenumber m space. $\mathcal{A}(m)$ can be decomposed into the clockwise (C) and anticlockwise (A) components by forming:

$$C(m) = \frac{1}{2}\overline{\mathcal{A}(-m)\mathcal{A}^*(-m)} \tag{6}$$

and

$$A(m) = \frac{1}{2}\overline{\mathcal{A}(m)\mathcal{A}^*(m)} \tag{7}$$

where the overbar means an average over all spectra and * is the complex conjugate. The total energy is

$$E(m) = A(m) + C(m) \tag{8}$$

The ratio $r_n(m) = C(m)/E(m)$ ($r_s = A(m)/E(m)$) gives the sense of vertical propagation at a particular wavenumber, remembering that winds associated

with upward propagating waves rotate clockwise (anticlockwise) with height in the northern (southern) hemisphere. A value greater than 0.5 indicates more energy is going up than down. Of more interest usually is the ratio averaged over all relevant wavenumbers, for example $r = \overline{C(m)}/\overline{E(m)}$. Radiosonde and rocket measurements all show that energy is primarily upward going in the stratosphere with $r \sim$70-80%, which shows that the main wave sources are in the troposphere.

3.2 Horizontal propagation directions

Polarization relation (2) is simplified by rotating the coordinated system to align the axes with the major and minor axes of the perturbation ellipse. If $u'_{\parallel}$ and $v'_{\perp}$ are the horizontal perturbation velocities parallel and perpendicular to the wave vector then (2) becomes

$$v'_{\perp} = -i\frac{f}{\hat{\omega}}u'_{\parallel} \qquad (9)$$

This expression shows that the intrinsic frequency $\hat{\omega}$ can be determined in terms of f from the axial ratio of the hodograph.

Furthermore, the horizontal direction of propagation of the wave is aligned along the major axis. In Figure 5a, for example, the major axis is aligned in the NE/SW quadrants, so inspection of the hodograph gives the propagation direction, at least with a 180° ambiguity.

In practice, it is not quite so simple to deduce the intrinsic frequency and direction of propagation from the hodograph. A spectrum of waves will generally be present, each with a with different azimuth of propagation, and the background wind will change with height, changing the intrinsic frequency. A more quantitative, statistical, description of gravity wave motions is obtained by making an analogy between partially polarized gravity wave and electromagnetic wave fields. Vincent and Fritts (1987) introduced the concept of Stokes parameters, which allow the degree of polarization and alignment of the polarized component to be determined. Initially the technique was applied to time series of wind motions. Eckermann and Vincent (1989) ex-

tended the idea to vertical wind profiles where in vertical wavenumber space. The Stokes parameters are defined as:

$$I = \overline{u'^2} + \overline{v'^2} \tag{10}$$

$$D = \overline{u'^2} - \overline{v'^2} \tag{11}$$

$$P = 2\overline{u'v'cos\delta} \tag{12}$$

$$Q = 2\overline{u'v'sin\delta} \tag{13}$$

The parameters I, D, P, and Q have simple interpretations. I is the total energy in the spectrum, while D and P are measures of the anisotropy of the field. The parameter Q gives the sense of rotation of the polarization ellipse (positive is clockwise and negative is anticlockwise). With these parameters it is easy to calculate the phase difference, δ, major axis orientation, ϕ, and ellipse axial ratio, AR, of the elliptically polarized wavefield:

$$\delta = tan^{-1}\left(\frac{Q}{P}\right) \tag{14}$$

$$2\phi = tan^{-1}\left(\frac{P}{D}\right) \tag{15}$$

$$AR = cot\xi \quad \text{where} \quad 2\xi = sin^{-1}\left(\frac{Q}{dI}\right) \tag{16}$$

$$d = \frac{(D^2 + P^2 + Q^2)^{1/2}}{I}. \tag{17}$$

The quantity d is the degree of polarization, which indicates the ratio of polarized to irregular motions. Note, sufficient averaging in either frequency or wavenumber space is required in order to ensure estimates of d are statistically reliable (Eckermann and Vincent, 1989). Values of d range between 0

(unpolarized) to 1 (polarized); intermediate values imply a partially polarized wave field. In typical radiosonde soundings it is not unusual to obtain values of $d \sim 0.5$ or larger (Vincent and Alexander, 2000).

Additional information is required to resolve the 180° directional ambiguity. This can be achieved if w' is measured. The polarization relation linking w' to $u'_\parallel$ is

$$w' = -\frac{k_h}{m}u'_\parallel \tag{18}$$

The upward flux of horizontal momentum $\overline{u'_\parallel w'} = -(k_h/m)\overline{u'^2_\parallel}$ has the same sign as k_h for upward propagating waves ($m < 0$). In component terms, the relevant fluxes are $\overline{u'w'}$ and $\overline{v'w'}$.

Specialized radar techniques allow momentum fluxes to be measured directly so that directions can be ascertained. Normally, however, it is neither possible to measure momentum fluxes directly, nor to compute them indirectly due to difficulties in measuring the small values of w'. An alternative approach is to use temperature as a surrogate for w'. Kitamura and Hirota (1989), Hamilton (1991), and Vincent et al (1997) showed how the relative phase of temperature and horizontal wind perturbations can be used to determine the sense of horizontal phase progression. $\hat{T}'$ is related to $u'_\parallel$ via

$$\hat{T}' = \mp i\frac{N^2}{g\hat{\omega}}\frac{k_h}{m}u'_\parallel, \tag{19}$$

where the negative sign is chosen when $km > 0$ and the positive sign when $km < 0$. The $i = \sqrt{-1}$ factor means that the horizontal motions are 90° out of phase with the temperature perturbations. Figure 5b shows the relationships between the three quantities for the case where $k_h > 0$ so that u' and w' are in phase (i.e. $\overline{u'_\parallel w'} > 0$). Coldest temperatures lag a quarter cycle after maximum upward (positive) velocities.

Rearranging (18) and (19) gives

$$\overline{u'w'} = \frac{\hat{\omega}g}{N^2}\overline{u'_\parallel \hat{T}'_{+90}} \tag{20}$$

where $\hat{T}'_{+90} = i\hat{T}'$ is obtained by first Hilbert transforming $\hat{T}'$ in the appropriate sense and then reverse transforming to produce a 90° phase shift in $\hat{T}'$ at all spatial frequencies without changing the amplitude (Vincent et al., 1997). Alternatively, the quadrature spectrum between $u'_{||}$ and $\hat{T}'$ can be used; where velocity components are available then $u'\hat{T}'_{+90}$ and $v'\hat{T}'_{+90}$ are the relevant quantities. Examples of the distributions of horizontal propagation directions (angular spectra) determined by this technique from radiosonde observations in the tropical lower stratosphere are shown in Figure
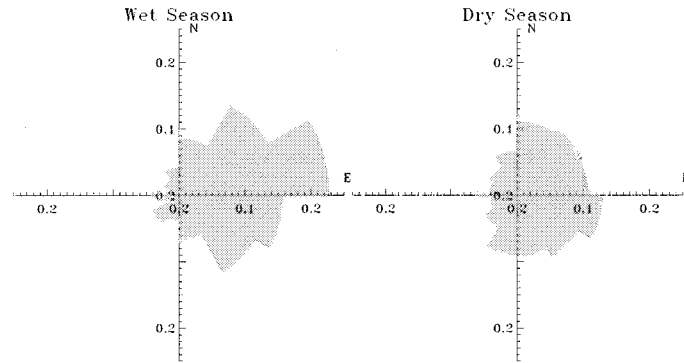
ƒ

ς

Figure 6: Angular spectrum of gravity waves observed in the 18-25 km height range over Cocos Island (after Vincent and Alexander, 2000)

While it is useful to use the sign of (20) to obtain the direction of propagation it is less useful for determining momentum fluxes, since $\hat{\omega}$ is required. There is no unambiguous way of determining this quantity from observations alone because it is not always clear whether the fluctuations measured by radiosondes and rockets, for example, are due to a wide spectrum of waves or are dominated by a quasi-monochromatic waves. This issue is explored further by Vincent and Alexander (2000) and Alexander and Vincent (2000).

4 Momentum Fluxes

As gravity waves propagate into the atmosphere their amplitudes grow as $\sim exp(-z/2H)$ in order to conserve energy. For conservative motions the momentum flux $\overline{\rho u'w'}$ remains constant. Where the flux changes there is an associated body force, which in equatorial regions where the Coriolis force is low, leads to an acceleration of the zonal flow (see lectures by Hamilton). In order to understand and quantify the role of gravity waves it is important to measure momentum fluxes and their change with height. The techniques using temperature described above are not very satisfactory. First, there is poorly known value of $\hat{\omega}$ in (20). Secondly, there is the issue of observational selection or filtering in which techniques can only view or select parts of the wave spectrum. This issue is discussed further in section 6.
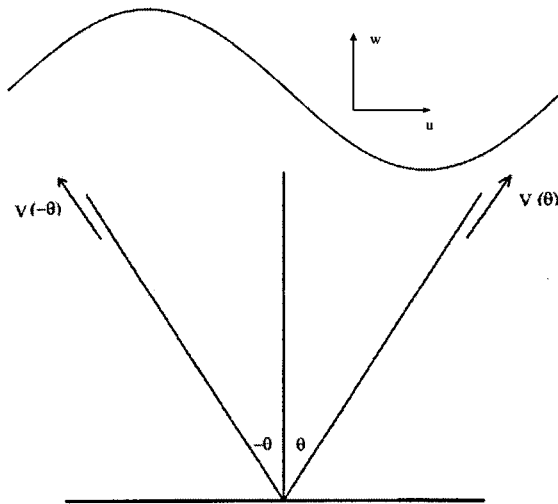

Figure 7: Configuration of the complementary dual-beam radar technique for measuring momentum fluxes (see text).

A direct way of measuring momentum fluxes is to use Doppler radars. Figure 7 shows the configuration which uses two narrow beams. One points at an angle θ to the zenith and the other points in the complementary direction,

$-\theta$. The radial velocity along the first beam at range R is

$$v_r(\theta, R) = u'sin\theta + w'cos\theta \tag{21}$$

and for the complementary beam

$$v_r(-\theta, R) = u'sin\theta - w'cos\theta \tag{22}$$

Squaring and adding equations (21) and (22) and rearranging gives (Vincent and Reid, 1983)

$$\overline{u'w'}(z) = \frac{\overline{v_r^2(\theta, R)} - \overline{v_r^2(-\theta, R)}}{2sin2\theta} \tag{23}$$

so that the momentum flux can be measured at different heights, z. By steering beams in the EW and NS plans it is possible to measure both $\overline{u'w'}$ and $\overline{v'w'}$. This has proved a robust technique, but there some requirements that restrict its use. One problem is that the fluxes are derived from small differences in radial velocities, which requires very accurate measurements.

Another important factor is the need to know the pointing angles accurately, so narrow beams are required. This means large radars. At MF the only radar with the capability is the 1-km diameter array at Buckland Park near Adelaide. At VHF the largest and most powerful MST radars can also exploit the technique. These include the MU radar in Japan, the Jicamarca radar in Peru and the MST radar in Tirupati, India.

Despite these limitations the technique has been used to test and verify predictions about wave mean-flow interactions, including interaction between gravity waves and tides (Fritts and Vincent, 1987) and wave-driven circulations. So far the technique has had limited use for studying wave mean flow interactions at the equator, where gravity waves are thought to play a major role in forcing the QBO and mesospheric SAO. In order to explore the role of gravity waves in driving circulations at the equator a new MF radar is under construction at Pontianak in Indonesian West Kalimantan (0°, 109°E). This is a region of strong convection, probably the major source of gravity waves in the tropics.

5 Gravity Wave Spectra

A convenient way to summarize information about gravity waves is by computing spectra of their observed parameters. Spectra in frequency and wavenumber space show approximately invariant forms, despite the exponential decrease of density with height and regardless of season or geographic location. It was originally argued by VanZandt (1982) that there was a "universal" spectrum of atmospheric gravity waves, in analogy with internal wave spectra in the oceans. There has been vigorous debate about the mechanisms that constrain the wave motions and several "saturation" theories have been proposed. There is also debate as to whether the spectra have "universal" amplitudes (to within a factor of two) at all locations, although observations do show some degree of universality of slope.

5.1 Frequency spectra

Long time sequences of winds measured by radars lend themselves to ease of compution of frequency frequency. Irrespective of whether observations are made in the lower or upper atmosphere the spectra have a common form $S(\omega) \sim \omega^{-p}$, where ω is the observed frequency measured in a ground-based frame. The spectral index is usually $p \sim 3/2 - 5/3$. Spectra derived MF radar observations of winds measured at the mesospause (~ 85 km) with MF radars situated at the equator show a characteristic $\omega^{-5/3}$ shape, at least at periods shorter than about 1 day. At longer periods the motions are dominated by the effects of planetary-scale waves (Kovalam et al, 1999).

A complication with frequency spectra derived from ground-based observations is that they are determined in terms of ω and not intrinsic fequency, $om\grave{e}ga$. Recent observations made with constant pressure balloons floating at almost constant heights near 20 km do not suffer from this limitation, however. The balloons, drifting under the influence of the mean winds and waves, act as Lagrangian tracers so that the horizontal and vertical motions are measured in intrinsic coordinates. Spectra computed from long-term
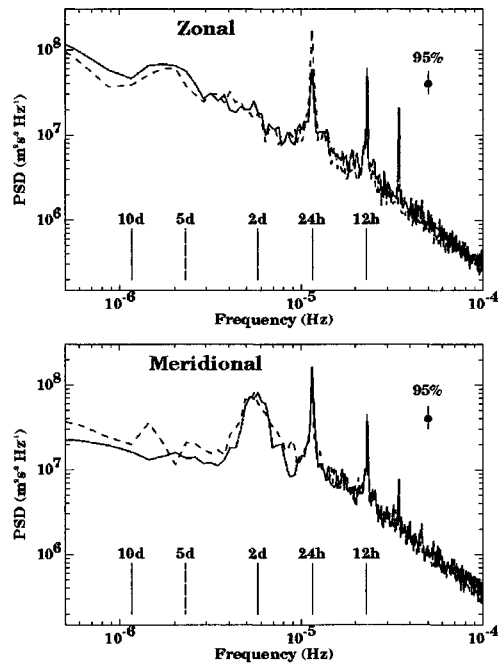
Figure 8: Frequency spectra of hourly averaged zonal (top) and meridional winds (bottom) averaged between 86 and 92 km at Christmas Island (solid line) and Pontianak (dashed line) for the period November 1995 to August 1997. Confidence limits at the 95% level are indicated.

(several day) observations at both the equator and Arctic show $S(\hat{\omega}) \sim \hat{\omega}^{-2}$
(F. Vial, Personal Communication, 2001).

5.2   Vertical wavenumber spectra

Studies made with many different techniques over heights ranging from the
troposphere to the lower thermosphere give broadly similar descriptions of
vertical wavenumber spectra. At high wavenumbers they show spectra of the
form $F(m) \sim m^{-t}$ with t in the range 2 to 3 [e.g. Smith et al., 1987]. There
have been many different attempts to provide a theoretical basis for this
functional form based on a saturation process that limits wave growth. For
example, Dewan and Good (1986) proposed a saturation limit imposed by
convective or dynamical instability and argued that saturated waves should
have spectra with an N^2/m^3 dependence.

At low wavenumbers (long vertical wavelengths) the waves need not be
saturated and can grow with height. The transition between between satu-
rated and unsaturated waves occurs at some characteristic wavenumber m_*.
Smith et al (1987) gave a simple function form for the m spectrum as

$$F(\mu) = \frac{\mu^2}{1 + \mu^{s+t}} \tag{24}$$

where $\mu = m/m_*$ is a constant and $t = 3$. The spectral index for the low
frequency part of the spectrum is difficult to measure, but is often taken as
$s = 0$. This kind of spectrum is often referred to as the modified-Desaubies
spectrum. A diagram encapsulating many different data sets taken in dif-
ferent regions of the atmosphere is shown in Figure 9. Based on radar
observations in the troposphere and lower stratosphere, radiosonde, rock-
etsonde, GPS/MET and lidar observations in the stratosphere, and radar
and lidar observations in the mesosphere the characteristic vertical wave-
length $\lambda_* = 2\pi/m_*$ increases from about 2 km in the troposphere to about
16-20 km at the mesopause. Some observations, notably lidar observations
in the middle stratosphere, show amplitudes that are below saturation lim-
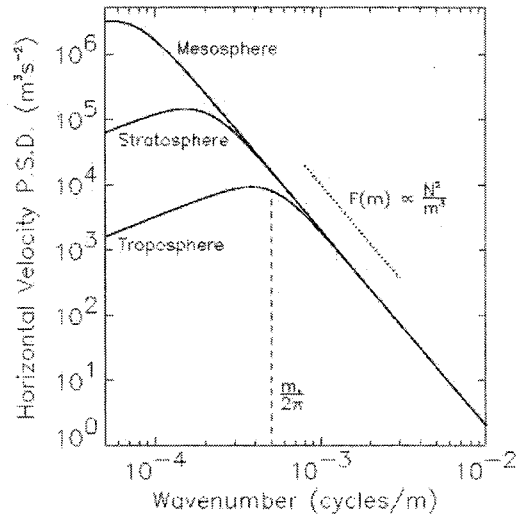its. Eckermann (1995) discuss the physical processes that can lead to these

Figure 9: The modified-Desaubies spectrum of horizontal wind fluctuations in different atmopsheric regions (after Smith et al., 1987).

attenuated spectra.

6 Observational Selection

As waves propagate in a height varying background wind the intrinsic frequency $\hat{\omega} = \omega - k_h\bar{u}$ will change, which impacts on which waves can be observed. To better understand the process it is useful to use a simplified form of the dispersion relation

$$|m| \sim \frac{N}{\hat{\omega}}k_h \sim \frac{N}{|\bar{u} - c|} \tag{25}$$

where c is the ground-based wave frequency. Figure 10 taken from Alexander (1998) helps with visualizing how Doppler shifting can effect m, depending on whether a wave is propagating against or with the mean flow. Eckermann (1995) and Alexander (1998) discusses the importance of the Doppler-shifting effect when an instrument or technique can only respond to waves in a certain range of m or vertical wavelength. This is equivalent to an observational
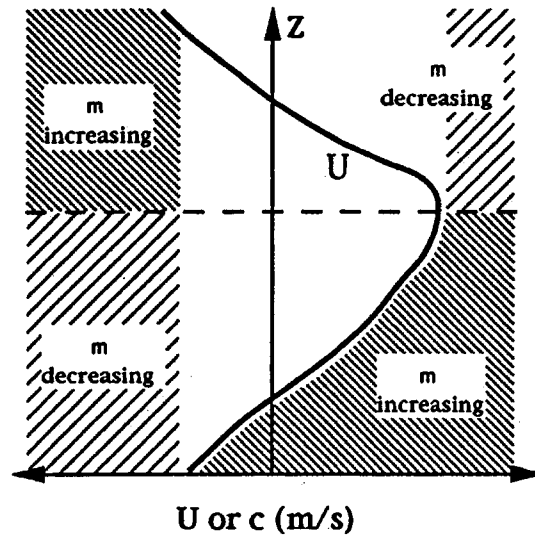
Figure 10: Schematic diagram showing the Doppler shifting effects of the mean wind on vertical wavenumber m (after Alexander, 198).

filter, as exemplified in Figure 11 for radiosondes, rockets and the microwave limb sounder (MLS) instrument on UARS. At one extreme radiosondes "see" short wavelength waves, while MLS is sensitive to waves with long vertical wavelengths. Waves will move in or out of the observational window in height regions where there are strong shears in background wind, so observed changes in wave amplitude may be more apparent than real. Ground-based instruments, such as radars and lidars, will suffer a similar effect as changing background winds Doppler-shift wave energy in frequency (Fritts and VanZandt, 1987). Understanding how observational selection affects gravity wave studies requires careful analysis and modeling; all techniques are affected.
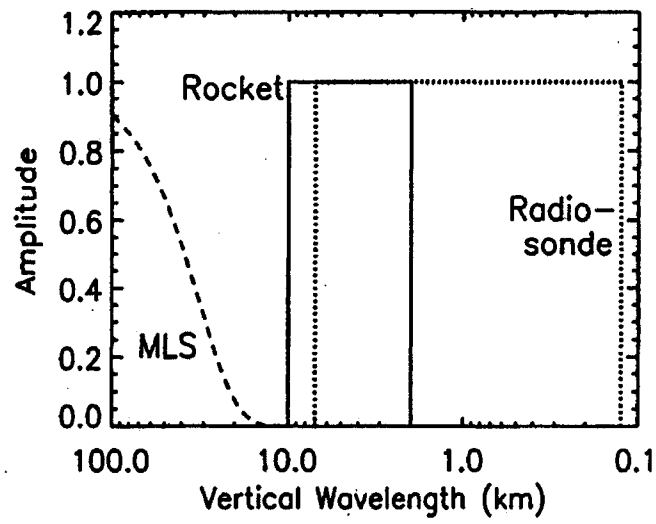
Figure 11: Observational filter functions showing fractional amplitude as a function of vertical wavelength for rocket sounding (solid), radiosondes (dotted) and Microwave Limb Sounder (MLS) (after Alexander, 1998).

References

[1] Alexander, M.J., Interpretations of observed climatalogical patterns in stratospheric gravity wave variance, *J. Geophys. Res.*, *103*, 8627-8640, 1998.

[2] Alexander, M.J., and R.A. Vincent, Gravity waves in the tropical lower stratosphere: A model study of seasonal and interannual variability, *J. Geophys. Res.*, *105*, 17,971-17,982, 2000.

[3] Allen, S.J., and R.A. Vincent, Gravity wave activity in the lower atmosphere: Seasonal and latitudinal variations, *J. Geophys. Res.*, *100*, 1327-1350, 1995.

[4] Dewan, E.M., and R.E. Good, Saturation and the "universal" spectrum for vertical profiles of horizontal scalar winds in the atmosphere, *J. Geophys. Res.*, *91*, 2742-2748, 1986.

[5] Eckermann, S.D., Effect of background winds on vertical wavenumber spectra of atmospheric gravity waves, *J. Geophys. Res.*, *100*, 14,097-14,112, 1995.

[6] Eckermann, S.D., and R.A. Vincent, Falling sphere observations of anisotropic gravity wave motions in the upper stratosphere over Australia, *Pure and Applied Geophys.*, *130*, 510-532, 1989.

[7] Fritts, D.C., and R.A. Vincent, Mesospheric momentum flux studies at Adelaide, Australia: Observations and a gravity wave/tidal interaction model, *J. Atmos. Sci.*, *44*, 605-619, 1987.

[8] Gardner, C.S., and W. Yang, Measurements of the dynamical cooling rate associated with the vertical transport of heat by dissipating gravity waves in the mesopause region at the Starfire Optical Range, New Mexico, *J. Geophys. Res.*, *103*, 16,909-16,926, 1998.

[9] Hamilton, K., Climatological statistics of stratospheric inertia-gravity waves deduced from historical rocketsonde wind and temperature data, *J. Geophys. Res., 96*, 20,831-20,839, 1991.

[10] Kitamura, Y., and I. Hirota, Small-scale disturbances in the lower stratosphere revealed by daily rawin sonde observations, *J. Meteorol. Soc. Japan, 67*, 817-831, 1989.

[11] Kovalam, S., R.A. Vincent, I.M. Reid, T. Tsuda, T. Nakamura, A. Nuryanto, and H. Wiryosumarto, Longitudinal variations in planetary wave activity in the equatorial mesosphere, *Earth, Planet. Sci., 51*, 665-674, 1999.

[12] Smith, S.A., D.C. Fritts, and T.E. VanZandt, Evidence for a saturated spectrum of gravity waves, *J. Atmos. Sci., 44*, 1404-1410, 1987.

[13] Tsuda, T., M. Nishida, C. Rocken, and R. Ware, Global Morphology of Gravity Wave Activity in the Stratosphere Revealed by the GPS Occultation Data (GPS/MET), *J. Geophys. Res., 105*, 7257-7274, 2000.

[14] VanZandt, T.E., A universal spectrum of buoyancy waves in the atmosphere, *Geophys. Res. Lett., 9*, 575-578, 1982.

[15] Vincent, R.A., Gravity wave motions in the mesosphere, *J. Atmos. Terr. Phys., 46*, 119-128, 1984.

[16] Vincent, R.A., and I.M. Reid, HF Doppler measurements of mesospheric gravity wave momentum fluxes, *J. Atmos. Sci., 40*, 1321-1333, 1983.

[17] Vincent, R.A., and D.C. Fritts, A climatology of gravity wave motions in the mesopause region at Adelaide, Australia, *J. Atmos. Sci., 44*, 1321-1333, 1987.

[18] Vincent, R.A., S.J. Allen, and S.D. Eckermann, Gravity-wave parameters in the lower stratosphere, in *Gravity wave processes: Their pa-*

rameterization in global climate models, (ed. K. Hamilton), pp. 7-25, Springer-Verlag, Berlin, 1997.

[19] Vincent, R.A., and M.J. Alexander, Gravity waves in the tropical lower stratosphere: An observational study of seasonal and interannual variability, *J. Geophys. Res.*, *105*, 17,971-17,982, 2000.